Available online at www.sciencedirect.com

ScienceDirect

Procedia Engineering 66 (2013) 565 – 574

Procedia Engineering

www.elsevier.com/locate/procedia

5th Fatigue Design Conference, Fatigue Design 2013

On the fatigue reliability of hydroelectric Francis runners

Martin Gagnon[a,*], Antoine Tahan[b], Philippe Bocher[b], Denis Thibault[a]

[a]*Institut de recherche d'Hydro-Québec (IREQ), 1800 Boulevard Lionel Boulet, Varennes, Québec, J3X 1S1, Canada*
[b]*École de technologie supérieure (ÉTS), 1100 Rue Notre-Dame Ouest, Montréal, Québec, H3C 1K3, Canada*

Abstract

The reliability assessment of large rotating structures like hydroelectric Francis runners is often limited by our capacity to define a proper limit state combined with a relevant degradation model. In this paper, we propose that the proper limit state for fatigue reliability of such structures is the onset of high cycle fatigue (HCF). Based on this premise, a prior interval for our limit state based on available literature is presented. The prior assumptions are believed to be the first step toward validation of the applicability and suitability of the proposed model. The paper includes an overview of the theoretical background for reliability assessment of Francis turbine runners, the methodology used, and the results obtained from the information gathered from the available literature.

Keywords: Reliability; High Cycle Fatigue (HCF); Hydroelectric turbine

1. Introduction

The capacity to define a proper limit state combined with a relevant degradation model is essential to the reliability assessment of large rotating structures such as hydroelectric Francis runners. Large Francis runners have a high downtime cost which limits inspection frequency. Since these structures can sustain a significant amount of damage without any safety issues, the main concerns are usually repair and downtime losses. Hence, for Francis runners, a crack needs to be repaired as soon as possible to minimize repair costs. Concurrently, the time between

* Corresponding author. Tel.: +1-450-859-8359; fax: +1-450-652-8905.
E-mail address: gagnon.martin@ireq.ca

doi:10.1016/j.proeng.2013.12.108

inspections must be maximized to reduce downtime. Combined, the inspection difficulty and long inspection interval leads to cracks that reach a detectable size only after the onset of High Cycle Fatigue (HCF).

Nomenclature

a	crack length
a_0	crack length at which the fatigue limit and the LEFM threshold cross
a_1	crack length at which behaviour deviate from the fatigue limit behaviour
a_2	crack length at which behaviour deviate from the LEFM threshold behaviour
$f_X(x)$	joint density function
$g(x)$	limit state
N	number of cycles
$N_{Startup}$	number of startup per day
N_{SNL}	number of regime change from maximum opening to SNL per startup
p	position of the defect
R	stress ratio
t	time
x	an n-dimensional vector of random variables
$Y(a)$	stress intensity correction factor for a given geometry
ΔK	stress intensity factor
ΔK_{th}	stress intensity factor of the LEFM threshold
ΔK_{onset}	stress intensity factor of the HCF onset
$\Delta\sigma$	stress cycle range
$\Delta\sigma_0$	fatigue limit
$\Delta\sigma_{LCF}$	stress cycle range of the LCF loading component
$\Delta\sigma_{HCF}$	stress cycle range of the HCF loading component
$\Delta\sigma_{Shutdown}$	stress cycle range of the shutdown transient
$\Delta\sigma_{SNL}$	stress cycle range of the regime change from maximum opening to SNL
$\Delta\sigma_{Startup}$	stress cycle range of the startup transient

The HCF onset is defined in this paper as the contribution to crack propagation of small amplitude stress cycles which are different from the high amplitude LCF cycles irrespective of their frequency [1]. We are faced with the following dilemma: if the HCF onset has occurred, longer time between inspections leads to a longer crack; yet, if an inspection is made before the HCF onset, we incur downtime and maintenance costs with limited and incomplete information on the state of the structure. Therefore, typical fatigue limit like the one derived from an SN curve or the detection of critical crack length are not suitable as they do not adequately reflect this reality and might result in excessive maintenance costs.

To circumvent these difficulties, we propose the use of the HCF onset as the limit state for reliability assessment. This approach relies on two assumptions:

- After the HCF onset, significant crack growth will be induced, the crack will become easily detectable and crack length will be linked to the time of operation rather than being a function of the number of Low Cycle Fatigue (LCF) events;
- If significant growth is expected, a crack needs to be repaired as soon as possible to minimize cost.

The thresholds below which the HCF loading does not contribute to crack propagation can be represented using the Kitagawa diagram [2]. This diagram combines two limits: the threshold for fatigue crack growth as define in the framework of Linear Elastic Fracture Mechanics (LEFM) and the fatigue limit for a given number of cycles which we assume to be 1E+07 cycles for material exhibiting an endurance limit. It should be noted that this diagram can also be extended to include more parameters such as notch effects and multi-axial criteria [3]. The methodology

developed [4] uses the limits formed by the Kitagawa diagram and the El Haddad correction factor [5] which accounts for short crack behavior as the limit state for the reliability assessment of large Francis turbine runners.

The paper is structured as follows: first we present our case study which is a run-of-the-river hydroelectric facility located in Quebec, Canada. Then, we describe the limit state used for reliability assessment followed by prior assumptions and discussion of the results obtained.

2. Hydroelectric Francis runner

Our case study is based on the Francis runner from a run-of-the-river hydroelectric facility in Quebec, Canada. This specific turbine runner was chosen because *in situ* measurements combined with historical operational data were both available. In this study, the studied location is a cutout near the runner crown present on each blade. This location was instrumented with strain gauges as shown in Figure 1.

The flaw geometries generally expected for such structures are either surface flaws or embedded flaws, as shown in Figure 2a. However, in our particular case, the critical zone is near the edge of the blade inside the cutout region. As a result, corner flaw geometry is a more representative geometry as shown in Figures 2b and 2c. In this paper, however, only the corner flaw in Figure 2c is studied in order to limit the number of random parameters considered. In this paper, the flaw stress intensity correction factor and crack growth data are taken from the BS7910:2005 [6].

A typical combined LCF+HCF loading is composed of an LCF component having a stress range $\Delta\sigma_{LCF}$ and a HCF component having a stress range $\Delta\sigma_{HCF}$, as shown in Figure 3a. Such a representation approximates the strain measured during a typical loading sequence (Figure 3b) if the startup and shutdown are neglected.

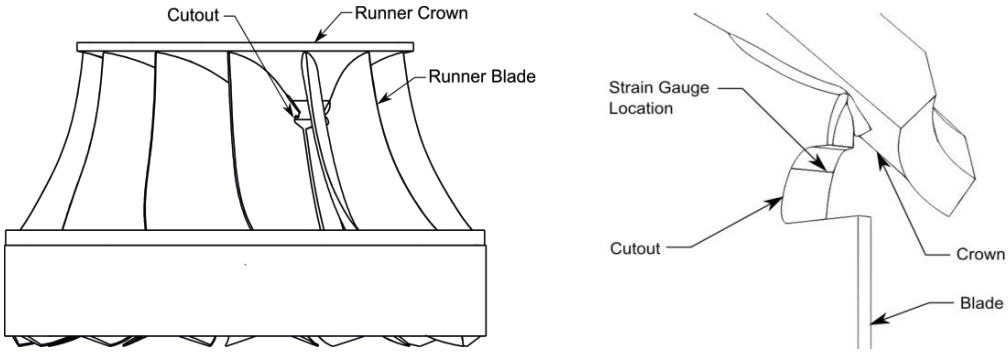

Fig. 1. Francis runner diagram. (a) Overall view of the runner; (b) Detailed view of the measured location.

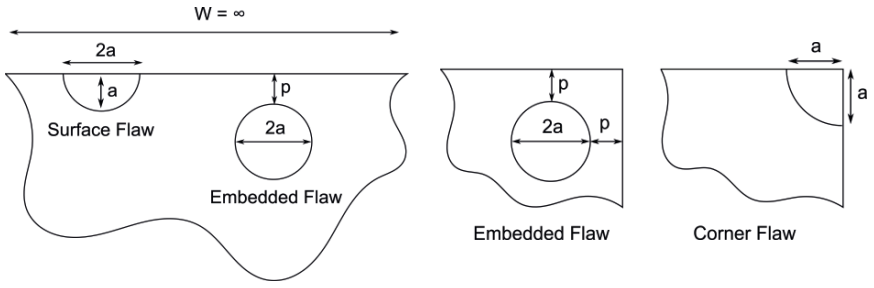

Fig. 2. Flaw geometries. (a) Typical surface and embedded flaw; (b) Corner embedded flaw; (c) Corner flaw.

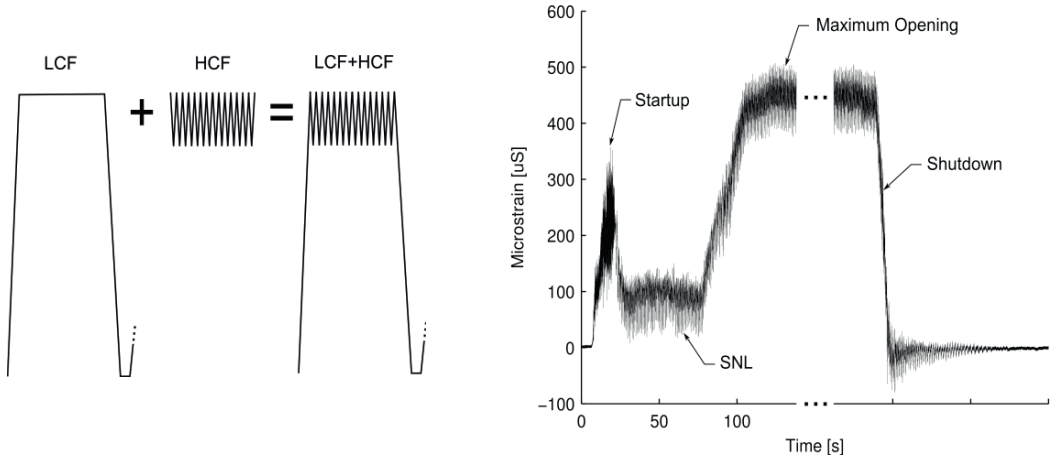

Fig. 3. (a) Schematic representation of combined LCF+HCF loading; (b) Measured loading during a typical loading sequence

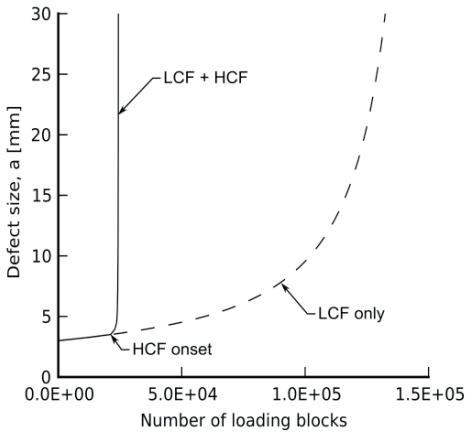

Fig. 4. Crack propagation comparison for HCF/LCF loading.

An example of the effect of the HCF loading compared to LCF crack growth is presented in Figure 4. We observed in this figure, using typical LEFM methodology from the BS7910:2005 [6], that the crack propagation results for LCF only, and combined LCF+HCF loading, are similar until the moment where the HCF component reaches the threshold for crack propagation. After this moment, the crack growth speed rises rapidly for the combined LCF+HCF loading.

However, transients like the one observed during startup have a significant influence on life expectancy, and are directly related to the control scheme used [7]. Hence, these transients need to be included in the load spectrum. A representation of the load spectrum used is shown in Figure 5 and the parameter values are presented in Table I. The load spectrum parameter values are considered representative of the strain range observed in the cutout location. Only two of the parameters are considered random: the initial defect size a and HCF stress range $\Delta\sigma_{HCF}$. Both parameters have an extreme value distribution and, even if their parameters values are plausible, they were chosen arbitrarily for illustrative purposes.

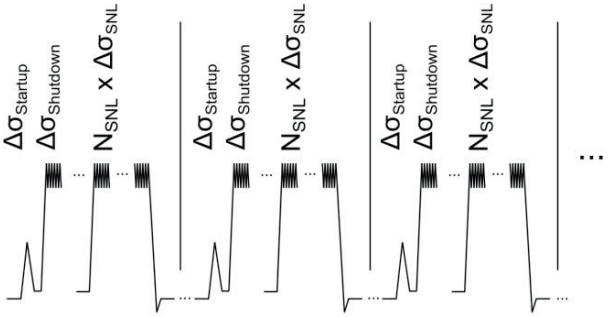

Fig. 5. Case study load spectrum.

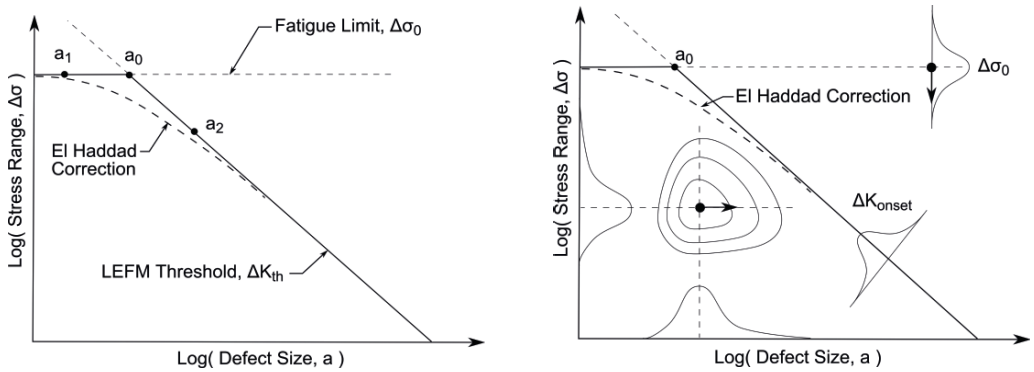

Fig. 6. (a) Schematic Kitagawa diagram; (b) Representation of the reliability problem.

Table 1. Case study parameter values.

Parameters	Location	Scale	Distribution type	Units
a	1.5	0.5	Gumbel	mm
$\Delta\sigma_{HCF}$	26.0	1.0	Gumbel	MPa
$\Delta\sigma_{Startup}$	70.0	-	-	MPa
$\Delta\sigma_{Shutdown}$	120.0	-	-	MPa
$\Delta\sigma_{SNL}$	100.0	-	-	MPa
$N_{Startup}$	0.232	-	-	Day−1
N_{SNL}	3	-	-	Startup−1

3. Limit state for HCF onset

For the reliability assessment of a structure, we need the following: a properly defined limit state model, a reliability criterion, and characterized uncertainty sources. In this study, the limit state is the HCF onset as proposed by Gagnon et al. [4]. This limit state is defined as the thresholds proposed by Kitagawa and Takahashi [2] combined with the correction factor developed by El Haddad et al. [5]. In this limit state, the El Haddad correction factor accounts for short crack growth by asymptotically matching the LEFM threshold and the fatigue limit. This limit state, commonly called the Kitagawa diagram, is shown in Figure 6a, and the uncertainties associated with the

parameters of the reliability problem are shown in Figure 6b. Notice the a1 and a2 points which represent the actual divergence from the fatigue limit and the LEFM thresholds where the El Haddad correction offers a conservative approximation [8].

In the Kitagawa diagram, the limit formed by the LEFM threshold is obtained from the stress intensity factor solution defined as follows:

$$\Delta K = \Delta\sigma\sqrt{\pi a}\; Y(a) \tag{1}$$

where ΔK is the stress intensity factor, $\Delta\sigma$ is the stress cycle range, a is the crack length and $Y(a)$ is the stress intensity correction factor for a given geometry. The limit state equation is obtained by replacing ΔK by the LEFM threshold ΔK_{th} in Eq. (1), which is rewritten as follows:

$$\Delta\sigma_{th} = \frac{\Delta K_{th}}{\sqrt{\pi a}\; Y(a)} \tag{2}$$

To capture short crack growth, El Haddad et al. [5] proposed to asymptotically match the limits defined by LEFM and the fatigue limit $\Delta\sigma_0$ using the reference crack length a_0 as a correction factor. The correction factor a_0 is added to the crack length a in Eq. (2) to obtain:

$$\Delta\sigma_{th} = \frac{\Delta K_{th}}{\sqrt{\pi(a+a_0)}\; Y(a+a_0)} \tag{3}$$

where the constant a_0 represents the transition between both limits, and is obtained by solving the following equation:

$$a_0 = \frac{1}{\pi}\left(\frac{\Delta K_{th}}{\Delta\sigma_0\; Y(a_0)}\right)^2 \tag{4}$$

For infinite life, $\Delta\sigma_0$ is the endurance limit. However, in cases where the limit for a finite number of cycles N is of interest, the number of stress cycles N can be accounted for by using the fatigue strength at N cycles rather than the endurance limit. Furthermore, it is relevant to note that all the parameters in Eq. (3) and Eq. (4) can be considered as independent random variables.

Finally, the criterion for failure needs to be expressed as follows:

$$g(x) \le 0 \tag{5}$$

with a probability of failure:

$$P_f = \int_{g(x)\le 0} f_X(x)\, dx \tag{6}$$

in which, x is an n-dimensional vector of random variables with a joint density function $f_X(x)$. Using Eq. (3) as the limit state, $g(x)$ becomes:

$$g(a,\Delta\sigma) = \Delta\sigma - \frac{\Delta K_{onset}}{\sqrt{\pi(a+a_0)}\; Y(a+a_0)} \tag{8}$$

If we consider a crisp limit state, our reliability model has two uncertainty sources: the defect size and the HCF stress range $\Delta\sigma_{HCF}$. However, as stated by Hall and Lawry [9] "… the distinction between 'failed' and 'not failed' states is seldom as crisp as the formulation of the limit state function suggests."

4. Prior limit state

Our objective is to define a range inside which we expect the limit state for the HCF onset to be located. The intervals obtained constitute prior assumptions which depend on the authors' opinions and information available. As such, they constitute priors that could be updated using Bayesian statistics to obtain less subjective posterior values [10]. Our limit state depends on two parameters: ΔK_{onset} and $\Delta\sigma_0$. Given that we currently don't have data for ΔK_{onset}, we will assume $\Delta K_{onset} = \Delta K_{th}$ for our prior. We present the data available in the literature for material similar to ASTM A-743 CA-6NM typically used for turbine runners in Table 2 and 3. This data constitutes the information available to establish our prior limit state interval.

Table 2. Threshold ΔK_{th} values from literature.

ΔK_{th} [MPa·m^{½}]	Description	Source
4.5	ASTM A-743 CA-6NM in water at R=0.1	Lanteigne et al. [11]
4.5	S41500, R=0.1, Air	Lanteigne et al. [12]
5.4	Cast SS 13Cr-4Ni, R=0.05, Water	Tanaka [13]
2.2	Cast SS 13Cr-4Ni, R=0.7, Water	Tanaka [13]
3.4	Cast SS 13Cr-5Ni, R=0, Dry Air	Usami and Shida [14]
6.0	Cast SS 13Cr-5Ni, R=0, Air	Usami and Shida [14]
5.1	Cast SS 13Cr-5Ni, R=0, Water	Usami and Shida [14]
2.3	Cast SS 13Cr-5Ni, R=0.5, Dry Air	Usami and Shida [14]
3.7	Cast SS 13Cr-5Ni, R=0.5, Air	Usami and Shida [14]
3.9	Cast SS 13Cr-5Ni, R=0.5, Water	Usami and Shida [14]
2.6	Cast SS 13Cr-5Ni, R=0.8, Water and Air	Usami and Shida [14]
2.0	Steels, including austenitic in air or other non-aggressive environments up to 100 °C	British Standards Institute [6]
$2.0 \leq \Delta K_{th} \geq 6.0\text{-}5.56R$	Steel	Hobbacher [15]

The values presented in Table 2 are taken from sources using different experimental protocols and methodologies. Among them, we also listed values from standards organizations and international body recommendations. The experimental data available do not allow us to define a most probable value or the probability distribution within this interval. Accounting for residual stress, we expected the HCF loading stress ratio to be around $R = 0.7$. The lowest reported value for that stress ratio is $\Delta K_{th} = 2.2$ by Tanaka [13]. However, both the BS7910:2005 [6] and the International Institute of Welding [15] recommend $\Delta K_{th} = 2.0$ as the lowest expected value for high stress ratio. Given the data available, $\Delta K_{th} = 2.0$ is considered as the lowest expected value for the HCF onset. On the other hand, we observe that the highest measured value is $\Delta K_{th} = 6.0$ at $R = 0$ reported by Usami and Shida [14] Accounting for some uncertainty, we can define the ΔK_{onset} prior at $R \geq 0.5$ to be within the interval [2.0, 6.0] MPa·m^{½}.

Table 3. Fatigue strength (stress range) $\Delta\sigma_0$ from literature.

N=1e7	N=1e11	Description	Source
410 MPa	198 MPa	ASTM A-743 CA-6NM in water, R = 0	Mahnig et al. [16]
135 MPa	55 MPa	ASTM A-743 CA-6NM in water corrected for P=95% and Smax = Su	Mahnig et al. [16] corrected by the authors
246 MPa	96 MPa	Steel with UTS < 552 MPa	ASME Section VIII Division 2 [17]
123 MPa	154 MPa	Steel with UTS = 793-892 MPa	ASME Section VIII Division 2 [17]

For the fatigue strength $\Delta\sigma_0$, we can only refer to the study by Mahnig, 1974 for our material ASTM A-743 CA-6NM. Furthermore, none of the sources listed in Table 3 report values for N=1E11 which is the maximum expected number of HCF cycles in our application. To circumvent this, the values have been linearly extrapolated by the authors. We consider such extrapolations to be conservative. For our lowest expected value, we used the values given by Mahnig et al. [16] corrected for a probability of 95% and for a maximum stress equal to the yield strength (550 MPa) using ASME methodology [18]. On the other hand, given the lack of experimental data, the yield strength is used for our upper limit. Our prior interval for fatigue strength $\Delta\sigma_0$ is [55, 550] MPa. By combining the prior interval for ΔK_{onset} and $\Delta\sigma_0$, we obtain the limits presented in Figure 6.

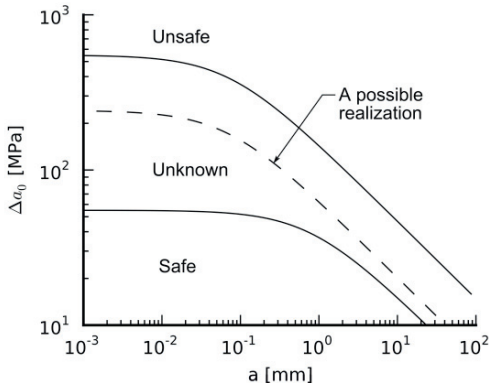

Fig. 6. Prior limit state interval.

The lower limit delimits a “Safe” region from an “Unknown” region inside which realizations of the limit state are expected to occur without any further information concerning value frequencies, probable values, distribution type, etc. The upper limit, on the other hand, delimits the region in which we are convinced that the HCF onset has occurred and the component is considered “Unsafe”. For practical purpose, the lower limit defines a region inside which, without knowing the actual safety factor, we believe that the HCF onset will not happen.

5. Results and discussion

The results obtained using the data in Table I, the limit state in Figure 6 and the LEFM methodology from the BS7910:2005 [6] for the contribution of the LCF loading to crack growth are presented in Figure 7. We observe that at t = 0 in Figure 7a, part of the joint distribution formed by the uncertainty in the HCF load $\Delta\sigma_{HCF}$ and defect size a cross the “Safe” state boundary and into “Unknown” state region. In the “Unknown” state region, the component can either be “Safe” or “Unsafe” without being able to assign a probability to each state. This is somewhat different from the typical reliability data where the component has either failed or not. We believe that using a prior interval is more suitable than a subjectively assigned distribution given the level of information available for our materials. However, one could argue that the bounds of our interval are also subjective. In such cases, the interval concept could be extended to a series of possible intervals in the form of a fuzzy set [19]. In the current study, we have

chosen to use only the interval concept for its simplicity and ease of interpretation. Observe in Figure 7b that the probability of being in the safe state diminishes from 90% to 82% after 100 years. Since the studied runner has 13 blades, the probability for the whole runner to be in the "Safe" region is $(90\%)^{13} = 26\%$ initially and diminishes to $(82\%)^{13} = 7\%$ after 100 years.

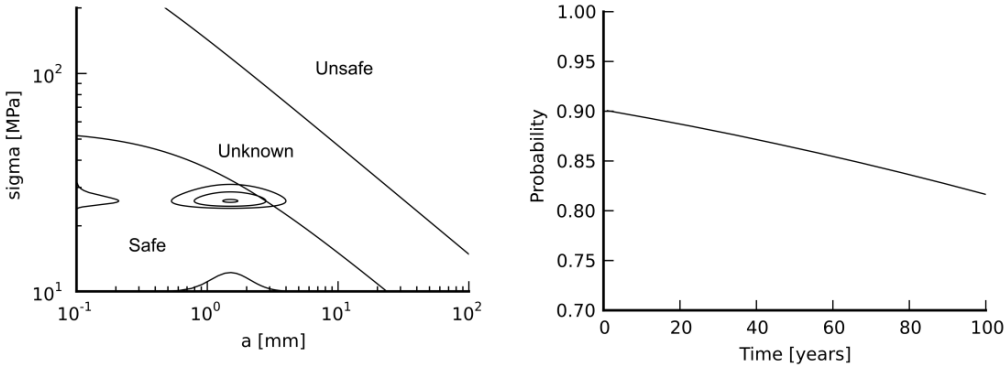

Fig. 7. (a) Initial problem $t = 0$; (b) Probability of the "Safe" state as of function of time.

6. Conclusions

The conclusions in this paper regarding the fatigue reliability of hydroelectric Francis runners are as follows:

- The loading of Francis runners can be decomposed in an LCF component which initially contributes to crack propagation and a HCF component which does not contribute initially to crack propagation.
- The operation of a Francis runner is considered "Unsafe" when the HCF loading component contributes to crack propagation.
- The limit state for the HCF onset is the thresholds proposed by Kitagawa and Takahashi [2] combined with the correction factor developed by El Haddad et al. [5]. This limit state is a function of both the HCF onset ΔK_{onset} and the fatigue strength $\Delta\sigma_0$.
- If we consider $\Delta K_{onset} = \Delta K_{th}$, we should expect the ΔK_{onset} for ASTM A-743 CA-6NM to be within the interval [2.0, 6.0] MPa·m^{½} given the data available in the literature.
- The $\Delta\sigma_0$ interval is defined as [55,550] MPa for ASTM A-743 CA-6NM given the data available in the literature.

We applied these using the loading observed on the runner from a run-of-the-river hydroelectric facility in Quebec, Canada. Our results show that the probability of being in the "Unsafe" state is negligible even after 100 years of operation. However, even in the initial state (t = 0) there is a significant risk of venturing into the "Unknown" state where we don't have enough information to discriminate between "Safe" and "Unsafe" states. Furthermore, this probability augments with time due to the LCF loading's contribution to crack propagation.

References

[1] T. Nicholas, *High Cycle Fatigue: A Mechanics of Materials Perspective*, Elsevier, 2006.
[2] H. Kitagawa, S. Takahashi, Applicability of fracture mechanics to very small cracks, in: *ASM Proceedings of 2nd International Conference on Mechanical Behaviour of Materials*, Metalspark, Ohio, pp. 627-631, 1976.
[3] E. Thieulot-Laure, S. Pommier, S. Fréchinet, A multiaxial fatigue failure criterion considering the effects of the defects. *International Journal of Fatigue*, 29(9–11), 1996–2004, 2007.
[4] M. Gagnon, A. Tahan, P. Bocher, D. Thibault, A probabilistic model for the onset of High Cycle Fatigue (HCF) crack propagation: Application to hydroelectric turbine runner, *International Journal of Fatigue*, 47, 300-307, 2013.

[5] M. H. El Haddad, T. H. Topper, K. N. Smith, Prediction of non propagating cracks, *Engineering Fracture Mechanics*, Vol. 11, pp. 573-584, 1979.
[6] British Standards Institute, *Guidance on some methods for the assessment of flaws in welded construction*, BS7910:2005, 2005.
[7] M. Gagnon, A. Tahan, P. Bocher, D. Thibault, Impact of startup scheme on Francis runner life expectancy, *IOP Conference Series: Earth and Environmental Science*, 12, 012107, 2010.
[8] D. Taylor, *Fatigue thresholds*, Butterworths (Canada) Limited, 1989.
[9] J. Hall, J. Lawry, Imprecise Probabilities of Engineering System Failure from Random and Fuzzy Set Reliability Analysis, 2nd International Symposium on Imprecise Probabilities and Their Applications, Ithaca, New York, 2001.
[10] J. K. Ghosh, M. Delampady, T. Samanta, An Introduction to Bayesian Analysis: Theory and Methods, Springer, 2007.
[11] J. Lanteigne, M. Sabourin, T. Bui-Quoc, D. Julien, The Characteristics of the Steels used in Hydraulic Turbine runners, IAHR 24th Symposium on Hydraulic Machinery and Systems, October 27-31, Foz do Iguassu, 2008.
[12] J. Lanteigne, M. Sabourin, T. Bui-Quoc, D. Julien, Comprehensive Research Program on Crack Propagation Characteristics of the Base Material used in Hydraulic Turbine Runners, WaterPower XV, hattanooga, USA, 2007.
[13] H. Tanaka, Studies on dynamic stress of runners for the design of 760 meter head pump-turbines, IAHR 16th Symposium, Sao Paulo, Brazil, 1992.
[14] S. Usami, S. Shida, Effects of Environment, Stress Ratio and Defect Size on Fatigue Threshold, *Journal of Japan Society of Materials Science*, Vol. 31, pp. 493-49,1982.
[15] A. Hobbacher, *Fatigue design of welded joints and components*, IIW-1303-95 (ex-doc. XIII-1539-96 / XV-845-96, Woodhead Publishing Limited, 1996.
[16] F. Mahnig, A. Rist, H. Walter, Strength and mechanical fracture behaviour of cast steel for turbines -Part One, *Water Power*, pp. 338-342, 1974.
[17] American Society of Mechanical Engineering (ASME), Boiler and Pressure Vessel Code, Section VIII, Division 2: Pressure Vessels, 2007.
[18] American Society of Mechanical Engineering (ASME), Criteria of the ASME Boiler and Pressure Vessel Code for Design by Analysis in Sections III and VIII, Division 2, 1969.
[19] M. Beer, M. Zhang, S. T. Quek, and S. Ferson , Structural Reliability Assessment with Fuzzy Probabilities, 7th International Symposium on Imprecise Probability: Theories and Applications, Innsbruck, Austria, 2011.